The global range of subduction zone thermal structures from exhumed blueschists and eclogites: Rocks are hotter than models

Sarah C. Penniston-Dorland [a,*], Matthew J. Kohn [b], Craig E. Manning [c]

[a] Department of Geology, University of Maryland, College Park, MD 20742, USA
[b] Department of Geosciences, Boise State University, Boise, ID 83725, USA
[c] Department of Earth, Planetary and Space Sciences, University of California, Los Angeles, CA 90095, USA

A B S T R A C T

The maximum-pressure P–T conditions (P_{max}–T) and prograde P–T paths of exhumed subduction-related metamorphic rocks are compared to predictions of P–T conditions from computational thermal models of subduction systems. While the range of proposed models encompasses most estimated P_{max}–T conditions, models predict temperatures that are on average colder than those recorded by exhumed rocks. In general, discrepancies are greatest for $P_{max} < 2$ GPa, where only a few of the highest-T model paths overlap petrologic observations and model averages are 100–300 °C colder than average conditions recorded by rocks. Prograde P–T paths similarly indicate warmer subduction than typical models. Both petrologic estimates and models have inherent biases. Petrologic analysis may overestimate temperatures at P_{max} where overprinting occurs during exhumation, although P–T paths suggest that relatively warm conditions are experienced by rocks on the prograde subduction path. Models may underestimate temperatures at depth by neglecting shear heating, hydration reactions and fluid and rock advection. Our compilation and comparison suggest that exhumed high-P rocks provide a more accurate constraint on P–T conditions within subduction zones, and that those conditions may closely represent the subduction geotherm. While exhumation processes in subduction zones require closer petrologic scrutiny, the next generation of models should more comprehensively incorporate all sources of heat. Subduction-zone thermal structures from currently available models appear to be inaccurate, and this mismatch has wide-reaching implications for our understanding of global geochemical cycles, the petrologic structure of subduction zones, and fluid–rock interactions and seismicity within subduction zones.

© 2015 Elsevier B.V. All rights reserved.

1. Introduction

Many important processes on Earth occur in subduction zones, including recycling of crustal materials and volatiles into the mantle, extraction of melts and creation of new crust that ultimately forms continents, and generation of some of Earth's deadliest earthquakes and chains of volcanoes. Subduction also provides a fundamental mechanism for geochemical cycling of materials among the different Earth reservoirs including atmosphere, hydrosphere, and lithosphere, and between crust and mantle. Our understanding of subduction zone processes and thermal conditions is informed by numerous sources, including observations from both active and ancient subduction zones. Observations of materials on the ocean floor and from arc volcanoes in active subduction zones provide a wealth of information about the materials entering and

leaving the subduction system. Geophysical observations such as seismic data provide constraints on characteristics such as the geometry of active subduction zones and provide a first-order idea of the materials within subduction zones. However the best way to directly study material that has been deep inside a subduction zone is to examine exhumed metamorphic rocks from ancient subduction zones. These rocks provide a "post-mortem" that allows us to determine the nature of materials within subduction zones and leads to a better understanding of processes occurring at depths beyond our direct observations.

Computational geodynamic models test our conceptual framework of subduction zone processes. The models use observations such as seismic data, spreading rates and heat flow to constrain model parameters, including slab geometry, thermal conditions, and convergence velocity. These models then provide predictions that can be tested by comparison with evidence from subduction-related metamorphic rocks. Models also provide the basis for quantitative estimates of geochemical cycling among Earth reservoirs of elements and compounds of great importance such as H_2O and
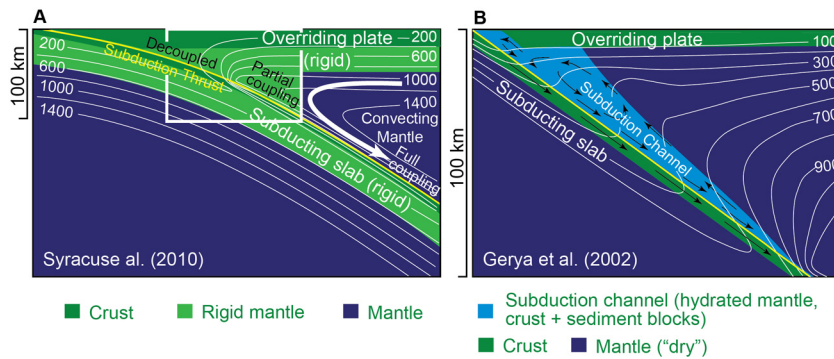
Fig. 1. Model parameters from **A.** Syracuse et al. (2010) and **B.** Gerya et al. (2002). White contour lines represent isotherms. White box in **A.** corresponds to size of **B.** (For interpretation of the color in this figure, the reader is referred to the web version of this article.)
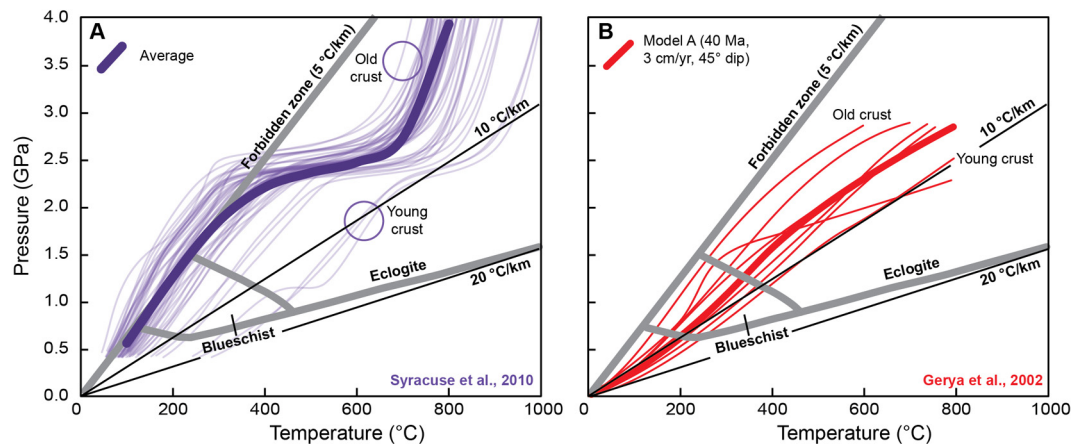

Fig. 2. *P–T* paths predicted for the top of the subducting slab. **A.** From Syracuse et al. (2010), updated van Keken (pers. comm., 2014) for currently active subduction zones (light purple lines). Darker line represents average of *P–T* paths. **B.** From Gerya et al. (2002). Light red lines represent *P–T* predictions based on varying a range of parameters including age of the incoming plate, subducting plate dip, viscosity of subduction channel, and convergence velocity. Darker red line represents an average subduction model (model A of Gerya et al., 2002) for a 40 Ma incoming plate with a 45 degree dip, a relatively low viscosity subduction channel, and a 3 cm/yr convergence rate. *P–T* conditions for blueschist and eclogite facies (Spear, 1993) along with a line indicating the boundary of the "Forbidden Zone" (Liou et al., 2000) shown in gray. (For interpretation of the color in this figure, the reader is referred to the web version of this article.)

CO_2 (e.g. Gorman et al., 2006; van Keken et al., 2011). The thermal structure of subduction zones provides an important control on the cycling of elements, as heat is a major driver of devolatilization reactions during subduction metamorphism.

The goal of this study is to compile and review pressure-temperature (*P–T*) conditions of exhumed, subduction zone metamorphic rocks to identify similarities and disparities in comparison with thermal models. We compare theory (models) with observation (rocks). We find that models consistently underpredict temperatures of exhumed rocks at *P* < 2 GPa and offer several possible explanations for this major disparity, including idiosyncrasies of exhumed rocks as well as model deficiencies. We then explore conceptually the corresponding implications of these explanations for cycling of volatile elements through the lithosphere and asthenosphere.

2. Approach

2.1. Introduction to models

Models of subduction zone thermal structures have examined the effects of varying factors that control temperature within subduction zones including convergence velocity, the age of the subducting plate, and the dip of the subducting plate. Many studies have modeled the thermal structure of subduction zones. Two relatively comprehensive modeling studies, Gerya et al. (2002) and Syracuse et al. (2010), are used for comparison to *P–T* estimates

from metamorphic rocks (Figs. 1, 2). These studies were chosen for two main reasons. First, both attempted to represent the range of *P–T* conditions that might be observed in the rock record. Second, they represent two endmembers in the range of predicted *P–T* conditions for subduction zones. Syracuse et al. (2010) generally predict *P–T* conditions on the cold end of the spectrum, whereas Gerya et al. (2002) predict *P–T* conditions on the hot end of the spectrum (see supplemental Fig. 1 for a comparison of these models to other subduction zone thermal models).

Syracuse et al. (2010) modeled the thermal structure within 56 segments of active subduction zones to obtain a suite of thermal models for the current global subduction system. This study followed the approach of van Keken et al. (2002) and used geometries of subducting slabs from each segment characterized by Syracuse and Abers (2006) and feature, from shallow to deep, 1) a shallow thrust zone with full slip of subducting slab beneath a fixed overlying plate, 2) at intermediate depths partial coupling between slab and overriding plate, and 3) at the deepest levels full coupling following four different assumptions about the causes of partial coupling (see Fig. 1A). In this study we use the preferred "D80" model in which the downdip end of partial coupling is at a constant depth of 80 km (Syracuse et al., 2010) as the baseline for comparison with *P–T* estimates from rocks. This model assumes that the corner of the fore-arc mantle in the overriding plate is cold (referred to as the 'cold nose') based on low heat flow measurements and low seismic attenuation. This model and others explain these physical observations through decoupling of the downgoing

plate from large-scale flow of asthenospheric mantle to depths of ∼80 km (e.g. Wada and Wang, 2009). The other three Syracuse et al. (2010) models result in similar or colder P–T estimates.

The range of P–T conditions predicted for the uppermost part of the basaltic oceanic crust of the 56 subduction segments of Syracuse et al. (2010), (updated van Keken, pers. comm., 2014; Fig. 2A) features a large number of relatively cold P–T paths that largely overlap, with a few higher-T paths predicted for subduction zones with very young oceanic crust (e.g. North and Central Cascadia). The assumption of full coupling of subducting slab and convecting overlying mantle at 80 km depth with no mantle convection at shallower levels results in a "shelf" in the P–T paths at 80 km (between ∼2 and 2.5 GPa) in which there is an isobaric temperature increase. An average D80 P–T path was calculated for all convergent boundaries based on these models. The average (dark line, Fig. 2A) is used as a baseline for comparison to P–T conditions recorded by metamorphic rocks.

Gerya et al. (2002) model a generic subduction zone and allow for self-organization of large-scale flow patterns of material within a region of relatively low viscosity that develops above the subducting slab – the subduction channel (see Fig. 1B). The configuration of this model is based on previous models of corner flow within the interface between subducting slab and overlying plate (e.g., Cloos, 1982) which were developed to explain the occurrence of subduction-related mélange terranes that contain relatively undeformed blocks of metamorphic rocks surrounded by a relatively fine-grained matrix. The geometry of the subduction interface is allowed to evolve over time as H_2O from dehydration reactions in the subducting slab rises and progressively serpentinizes the overlying mantle wedge, creating a relatively weak, flowing matrix. Gerya et al. (2002) investigated how variations in convergence velocity, incoming plate age, and subducting slab dip affected subduction zone thermal structure. Their "Model A" falls roughly in the middle of the range of P–T conditions predicted by their models, and is used as a baseline for comparison with rock P–T estimates (see Fig. 2B).

The sensitivity of the thermal structure to the age of the incoming plate, convergence velocity, and the dip of subduction was evaluated by van Keken et al. (2002) and Gerya et al. (2002). In general, younger (warmer) subducting plates possess higher predicted temperatures at a given pressure than do older plates (Fig. 3A), and slower convergence leads to higher temperatures for P < 2 GPa than does faster convergence (Fig. 3B). Slab dip makes little difference (Fig. 3C). Convection of material within the subduction interface (Gerya et al., 2002) substantially increases temperatures at shallower levels (P <∼2 GPa). Convection within the subduction channel mines heat from deep in the mantle and redistributes it along the top of the subducting slab, creating regular heating with increasing depth, whereas forced upper plate rigidity at depths of <80 km (Syracuse et al., 2010) leads to a drastic rise in temperature when the slab encounters convecting mantle. The nature of the overriding plate, whether oceanic or continental, does not appear to affect the thermal profile predicted by models. For example, while oceanic–continental subduction systems have slightly warmer average predicted temperatures than oceanic–oceanic systems (averaged from Syracuse et al., 2010), the age of the subducting plate in worldwide oceanic–oceanic systems is also somewhat older on average. Regression of model temperatures for specific depths against the age of the subducting plate, sediment thickness, nature of overriding plate, etc. yields indistinguishable results for oceanic–continental and oceanic–oceanic margins.

2.2. Compilation of P–T estimates from literature

Estimates of pressure and temperature were compiled from the literature from exhumed blueschists, eclogites, and associated
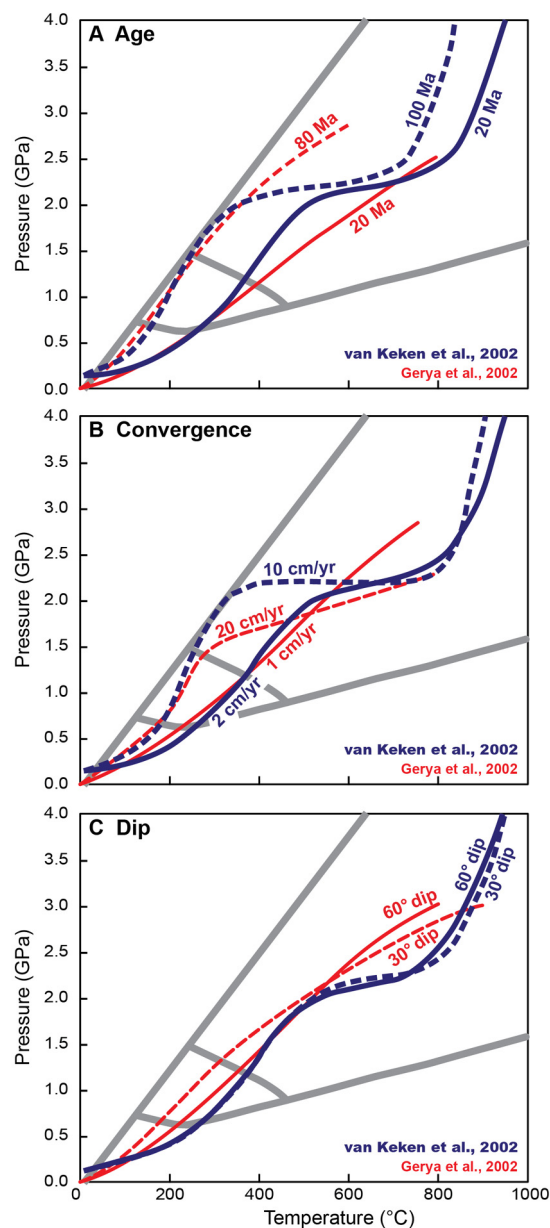

Fig. 3. P–T paths predicted for **A.** Differing ages of the incoming plate (Gerya et al., 2002, 3 cm/yr, 45° dip; van Keken et al., 2002, 2 cm/yr, 30° dip). Younger subducting oceanic crust is predicted to be hotter at a given depth compared to older subducting crust. **B.** Differing convergence velocities of the incoming plate (Gerya et al., 2002, 45° dip, 40 Ma plate; van Keken et al., 2002, 20 Ma, 30° dip). In general, slower convergence velocities are predicted to result in higher temperatures at a given depth compared to faster convergence velocities. **C.** Differing dip of the incoming plate (Gerya et al., 2002, 3 cm/yr, 40 Ma plate; van Keken et al., 2002, 2 cm/yr, 20 Ma plate). Plate dip is not predicted to exert a strong control on thermal structure. (For interpretation of the color in this figure, the reader is referred to the web version of this article.)

subduction-related metamorphic rocks from around the world. Only primary studies published in the last 25 years (1990 onward) were used for subduction systems younger than 750 Ma. These choices ensure greatest P–T accuracy and minimize potential thermal anomalies associated with Earth's secular cooling. The overall goal was to obtain the most accurate estimates of prograde P–T conditions for comparison with the P–T conditions predicted by the models. Accordingly, only the pressure and temperature estimates from the maximum P conditions recorded by the rocks were included. We refer to this condition as P_{max}–T. Usually these also correspond with maximum $T(T_{max})$. Although equilibrium as-
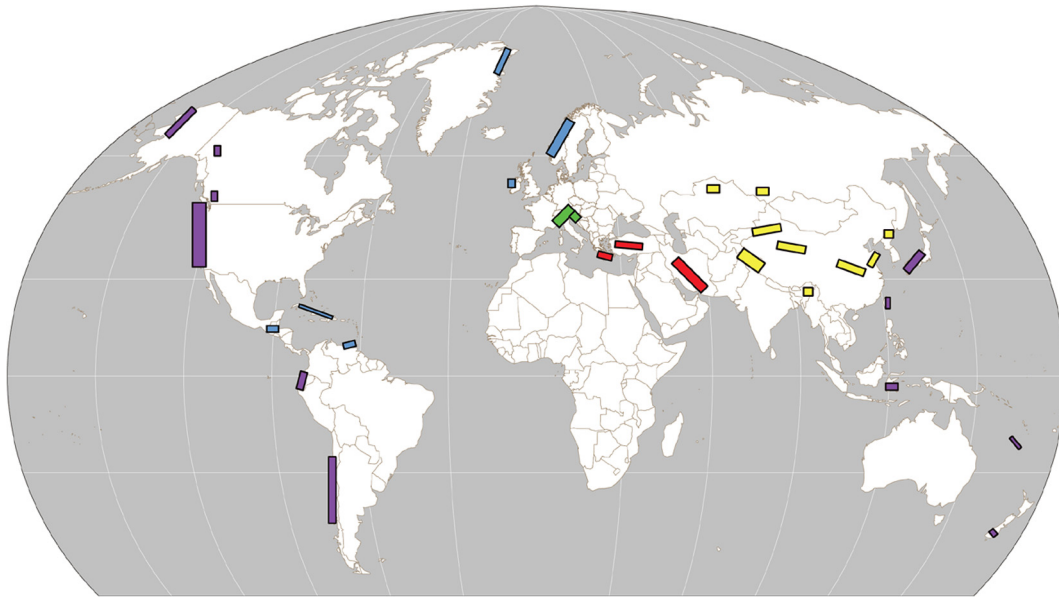
Fig. 4. Locations of studies around the world compiled from the literature for *P–T* estimates from metamorphic rocks. Colors on map correspond to colors of symbols from different regions depicted in Fig. 5. (For interpretation of the color in this figure, the reader is referred to the web version of this article.)

semblages are most confidently identified for P_{max}–T, chemically zoned minerals may also be used to infer the metamorphic *P–T* path. Thus, prograde *P–T* paths were compiled to assess thermal evolution during subduction. Values of P_{max}–T and *P–T* paths were derived either from calibrated thermobarometric equilibria (i.e. specific thermometers and barometers) or from phase equilibrium constraints on mineral stability fields, including pseudosections. This approach places important constraints on the extrapolation of published subduction thermal models for fluid production and element cycling in subduction zones. The P_{max}–T and prograde *P–T* path estimates cover a wide range of subduction conditions, including slow and fast convergence, old and young oceanic crust, and various subduction angles, in many ways analogous to the range of subduction conditions modeled by Syracuse et al. (2010). Fig. 4 shows the locations of the studies used in this compilation.

3. Comparison of model *P–T* predictions to exhumed rocks

The P_{max}–T estimates compiled from the literature fall dominantly within the metamorphic facies long identified with subduction zones: eclogite (both HP and UHP) and blueschist facies. A minority of *P–T* estimates fall within greenschist, epidote–amphibolite, prehnite-pumpellyite and zeolite facies (Fig. 5). For the total dataset, we estimate a global mean distribution of P_{max}–T conditions with 2σ confidence envelopes (Fig. 5F). For reasons discussed below, we propose that these conditions follow closely the *P–T* distribution along the subducting slab top (commonly referred to as the "subduction geotherm").

On average, P_{max}–T estimates at $P < 2$ GPa are hotter than average model predictions (Fig. 5). The average geothermal gradient at depths <70 km of the Syracuse et al. (2010) models is ~5 °C/km (Fig. 2A), far colder than that recorded by exhumed metamorphic rocks (Fig. 5). None of the rock P_{max}–T estimates, regardless of geographic region, overlap the model average; metamorphic temperatures are commonly 200 °C higher and range up to 400 °C higher than the model predictions. The shallow, cold *P–T* paths of Syracuse et al. (2010) fall in a region often referred to in metamorphic petrology textbooks as "not realized on planet Earth" (Spear, 1993), or alternatively as the "forbidden zone" (Liou et al., 2000; Hacker, 2006). Previous work (Hacker, 2006) estimated peak *P–T*

of ultra-high pressure (UHP) rocks and determined that no "robust" *P–T* determinations fall on the low *T* side of a 5 °C/km thermal gradient. Our survey affirms that "forbidden zone" conditions are not represented in the petrologic record of exhumed high-*P* rocks.

The model *P–T* predictions of Gerya et al. (2002) fall mostly within the range of conditions defined by the metamorphic facies commonly associated with subduction zones, following a path from zeolite to prehnite–pumpellyite to blueschist to eclogite facies conditions (Fig. 2B). Their reference Model A has an average thermal gradient of ~8 °C/km. As with the comparison to the Syracuse et al. (2010) predictions, comparison of the Gerya et al. (2002) predictions at <2 GPa reveals that rocks in our global compilation record temperatures that are higher on average. Only a few P_{max}–T estimates overlap with or are lower temperature than predicted by reference Model A of Gerya et al. (2002); most are ~100 °C higher and range up to 300 °C higher.

Where models include the deepest parts of subduction zone systems ($P > 2.5$ GPa), predictions compare favorably with P_{max}–T estimates from exhumed rocks. The data from natural systems are roughly equally distributed about the Syracuse et al. (2010) model predictions at these higher pressures. The models of Gerya et al. (2002) do not extend significantly to such high pressures, so comparisons are not possible.

At depths between 70–80 km – over the range of pressures where the "shelf" occurs in the Syracuse et al. (2010) models (i.e. 2 GPa < P < 2.5 GPa) – the mismatch between the model *P–T* predictions and the compiled *P–T* estimates from the literature diminish. The majority of *P–T* estimates still record hotter conditions for a given *P*, but some of the data points overlap with the Syracuse et al. (2010) average curve. This convergence in part reflects the "shelf" in the Syracuse et al. (2010) model *P–T* predictions, where a dramatic increase in temperature is predicted over this depth interval.

Prograde *P–T* paths (Fig. 6) generally corroborate the patterns indicated by P_{max}–T distributions in showing overall hotter conditions than are predicted by models. None of the prograde paths overlap with the Syracuse et al. (2010) model predictions for $P < 2$ GPa. Some of the prograde paths do overlap with the Gerya et al. (2002) model; however, paths are at higher *T* for a given *P*, and the prograde metamorphic record compares more favorably to the
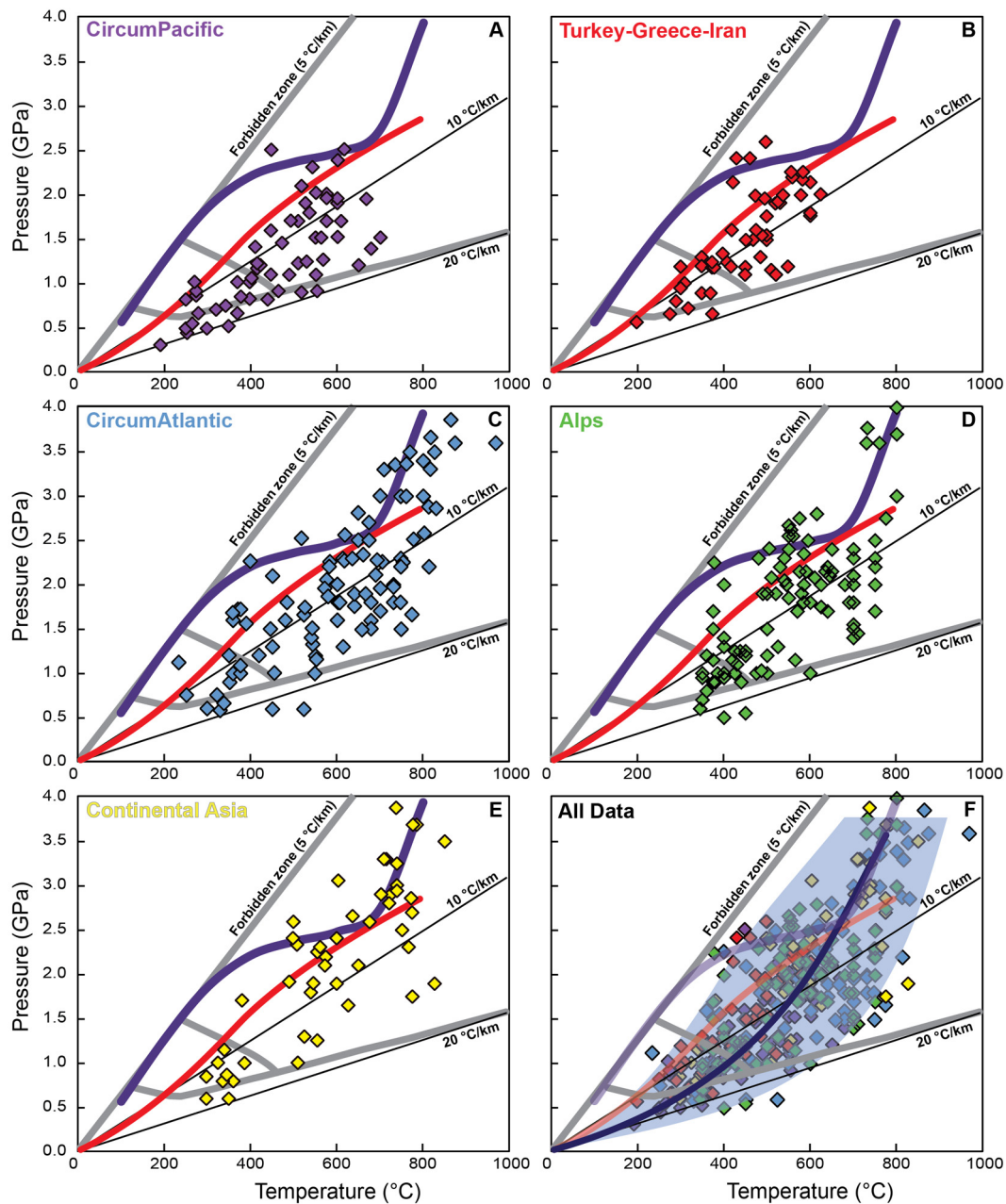
Fig. 5. Comparison of *P–T* estimates compiled from the literature to average model *P–T* predictions of Gerya et al. (2002) (solid red line) and Syracuse et al. (2010) (solid purple line) by region. **A.** CircumPacific, **B.** Turkey–Greece–Iran, **C.** CircumAtlantic, **D.** Alps, **E.** Continental Asia, **F.** *P–T* estimates from all locations plotted together with model averages. A global mean distribution of rock-based *P–T* estimates is shown (navy curve) with pale blue 2σ confidence envelopes. Model *P–T* predictions match the rock *P–T* estimates well for *P* > 2.5 GPa, however at shallower depths (<2 GPa) *P–T* estimates from metamorphic rocks at a given pressure are always hotter than the *P–T* predictions of Syracuse et al. (2010), commonly by more than 200 °C, and most are hotter than those predicted by Gerya et al. (2002). (For interpretation of the color in this figure, the reader is referred to the web version of this article.)

global mean distribution of *P–T* conditions (blue line and shaded region in Fig. 6F) than to the model predictions. A few paths evolve from cooler to warmer gradients, e.g. the well-studied blueschists and eclogites of Syros and Sifnos (Greece) exhibit nearly isobaric increases in *T* that result in a change in thermal gradient from ∼7 °C/km to ∼8 °C/km. Nearly all subduction *P–T* paths, however, evolve either along a nearly constant thermal gradient, or evolve from a warmer to cooler thermal gradient with a generally concave upward *P–T* trajectory. It is especially striking that the coherence between P_{max}–*T* conditions and models at UHP conditions (*P* > 2.5 GPa) reflects only P_{max}: early-stage *P–T* conditions of rocks that ultimately achieve UHP conditions are markedly hotter than model predictions.

4. Discussion

Overall, at depths of ∼70 km or less, exhumed high-P rocks record significantly hotter temperatures than are predicted by geodynamic models, both with respect to P_{max}–*T* conditions and early stages of *P–T* evolution. The discrepancy between the average temperatures for *P* < 2 GPa recorded by rocks and average temperature predicted by Syracuse et al. (2010) is greater than 200 °C and for Gerya et al. (2002) it is greater than 100 °C (Fig. 7). The differences in rock and the model temperatures of Syracuse et al. (2010) at *P* < 2 GPa are highly significant (t-test *p* values < 1 × 10^{-13}), and cannot be explained simply by population variances. These differences imply temperature gradients along the slab top that are higher than modeled by a factor of two for the
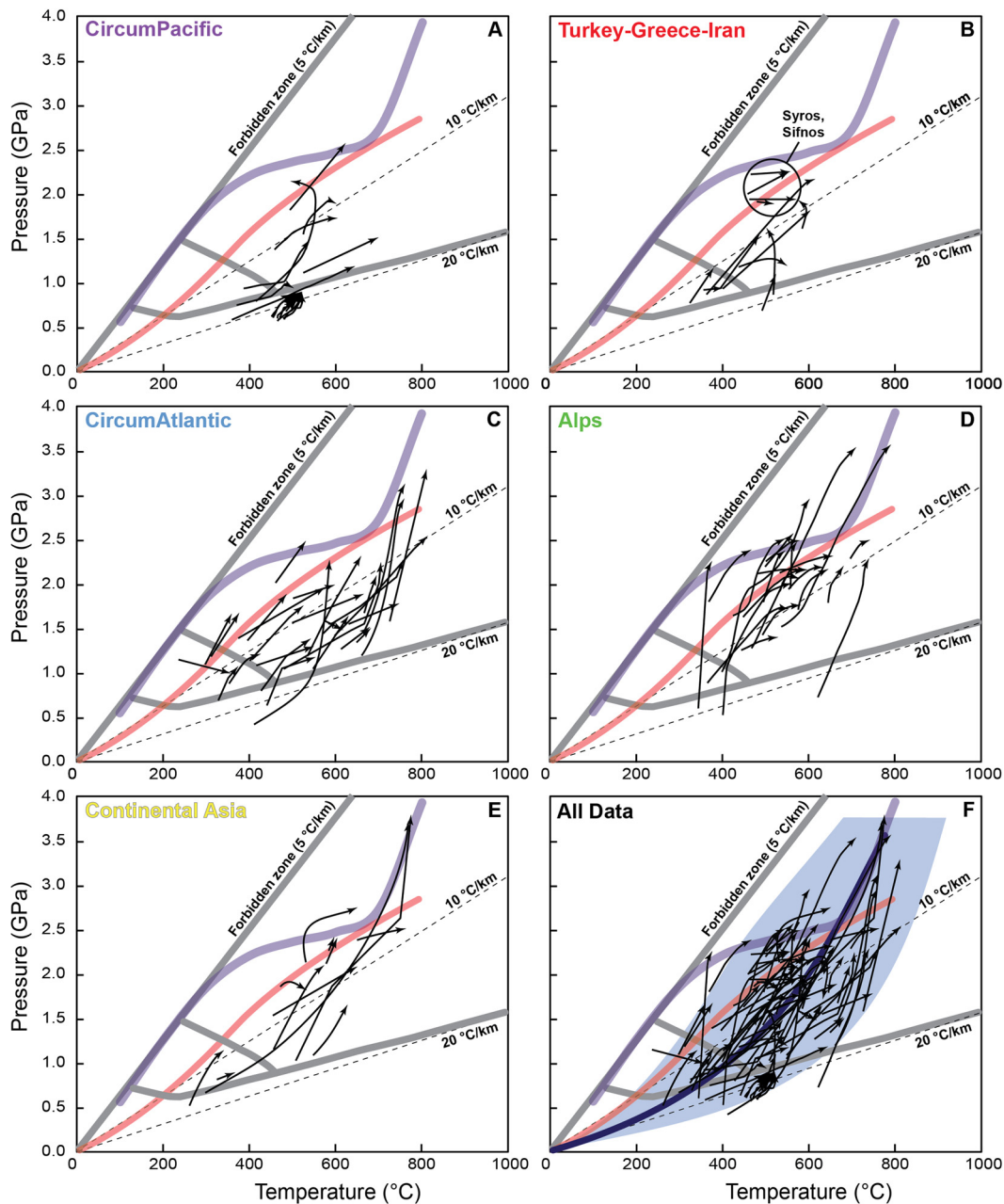
Fig. 6. Comparison of prograde *P–T* paths to average model *P–T* predictions of Gerya et al. (2002) (solid red line) and Syracuse et al. (2010) (solid purple line) by region. **A.** CircumPacific, **B.** Turkey–Greece–Iran, **C.** CircumAtlantic, **D.** Alps, **E.** Continental Asia, **F.** All locations with the global mean distribution of rock-based *P–T* estimates (navy curve) and 2σ confidence envelopes (pale blue) from Fig. 5. At shallow depths (<2 GPa) prograde *P–T* path estimates from metamorphic rocks are always hotter than the *P–T* predictions of Syracuse et al. (2010) and most are hotter than those predicted by Gerya et al. (2002). Although a few rocks do evolve towards a hotter thermal gradient (e.g. Syros and Sifnos), most evolve along a quasi-constant thermal gradient or towards a colder gradient. (For interpretation of the color in this figure, the reader is referred to the web version of this article.)

Syracuse et al. (2010) average and by ∼25% for the Gerya et al. (2002) reference Model A. The comparison to the Syracuse et al. (2010) model is particularly unfavorable – none of the *P–T* estimates from metamorphic rocks overlap with the average model *P–T* predictions, either at *P*_max–*T* or for the calculated prograde *P–T* paths. Below we explore reasons for the mismatch between *P–T* predictions from models and *P–T* estimates from metamorphic rocks.

4.1. Potential petrologic biases

One concern in data-model comparisons is the degree to which *P–T* conditions can be miscalculated or misinterpreted. Sources of

uncertainty in thermobarometric estimates include use of different phase equilibria, different endmember thermodynamic data (different calibrations), and different activity models. These differences can range up to 100 °C, for example several different calibrations have been proposed for the garnet-clinopyroxene Mg–Fe exchange thermometer (e.g., Powell, 1985; Krogh Ravna, 2000). Phase equilibrium errors are more difficult to constrain quantitatively, but thermodynamic databases and petrogenetic grids typically reproduce experimentally determined mineral stability fields and independent estimates of temperature to within ∼50 °C (for an example from Sifnos, Greece, see Fig. 8). In general *P* is not very dependent on *T*, for example typical barometers are not very temperature dependent (Krogh Ravna and Terry, 2004), thermometers
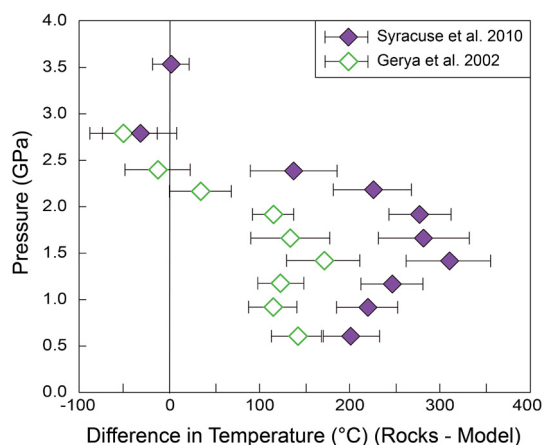
Fig. 7. Difference between rock and model T for specific pressures. Syracuse et al. (2010) refers to the average of the 56 models of modern subduction zones. Gerya et al. (2002) refers to their reference model A. Error bars for the Syracuse et al. (2010) comparison reflect 2 SE from both rocks and models. Differences are highly significant ($p < 1 \times 10^{-13}$) for all comparisons at $P < 2$ GPa. Error bars for the Gerya et al. (2002) comparison reflect 2 SE from the rocks alone because only one model is considered. Likewise p-values cannot be calculated for the Gerya et al. (2002). A comparison of the medians of these populations results in similar differences.
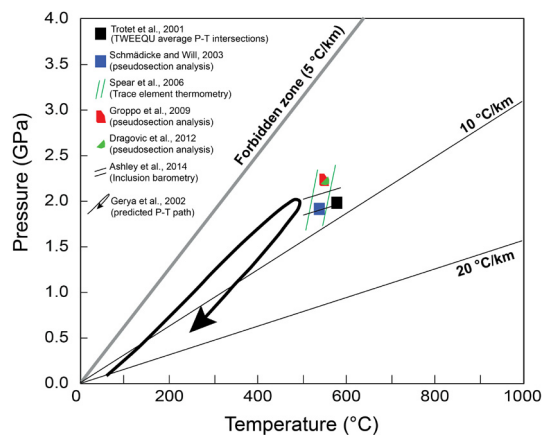

Fig. 8. Comparison of P–T estimates from the literature for subduction-related metamorphic rocks of Sifnos, Greece using different petrologic methods to estimate pressure and temperature conditions (Schmädicke and Will, 2003; Spear et al., 2006; Groppo et al., 2009; Dragovic et al., 2012; Ashley et al., 2014; Trotet et al., 2001). Predicted exhumation P–T path from Gerya et al. (2002). (For interpretation of the color in this figure, the reader is referred to the web version of this article.)

are not very pressure dependent, and mineral stability fields do not show much covariation between P and T.

Although these factors contribute uncertainty to P–T estimates from natural rocks, it is extraordinarily unlikely that use of different methods of computing P–T conditions are responsible for the discrepancy between rocks and models. First, thermobarometric and phase equilibrium uncertainties of 50–100 °C are smaller than the 200–300 °C difference observed between the P–T estimates from rocks and the model predicted P–T paths. Second, this argument requires all thermodynamic errors to overestimate temperatures, which is unlikely. Whereas considerable scatter can be observed in P_{max}–T conditions for an area (e.g. Alps; Fig. 5D), such scatter can be readily ascribed to combined differences in geography (different locations along the subduction system), and age (different times in the evolution of subduction), as well as petrologic error. The concave upwards distribution of P_{max}–T conditions might in part reflect systematic thermobarometric and pseudosection errors, but would require systematically higher calculated T at lower P, which has not previously been reported.

An additional source of geologic uncertainty is whether the mineral assemblages and compositions in the rocks reliably record conditions at P_{max}. Mineral assemblages in rocks typically preserve conditions corresponding to T_{max}, which do not necessarily occur at the peak pressure. In some cases, exhumation of rocks may lead to conditions under which minerals no longer record evidence of P_{max} – whether the rocks experience higher temperatures at lower pressures or isothermal decompression. These circumstances can lead to overprinting or eradication of high-pressure minerals or compositions. This phenomenon is sometimes invoked to explain the paucity of lawsonite eclogite assemblages (e.g. Whitney and Davis, 2006) whereby epidote-group minerals replace lawsonite. Our compilation of prograde P–T paths (Fig. 6), however, refutes this argument. Whereas a few rocks evolve towards warmer conditions (e.g. Syros and Sifnos, Fig. 6B), possibly explaining the replacement of lawsonite by epidote, most P–T paths actually trend roughly parallel to the envelope defined by P_{max}–T conditions (Fig. 5F). Thus the distribution of P_{max}–T conditions appears to be representative of subduction zone P–T paths.

Correspondence between P_{max} and T_{max} is consistent with the few models that include predictions for exhumation. For example, models of Gerya et al. (2002) predict that rocks in the subduction channel reach P_{max} and T_{max} simultaneously, close to the point of detachment from the top of the subducting slab (see Fig. 8). Although their study represents only one class of models, such results do suggest that rocks should faithfully record P–T conditions (T_{max}) close to the slab–mantle interface. Other oceanic subduction models do not intrinsically include exhumation so the corresponding modeled P–T paths experienced during exhumation cannot be discussed.

4.2. Potential model biases

Simplifications in model parameters can produce results that may not represent nature. Several factors that are not considered could cause models to predict unrealistically low temperatures at shallow depths, including the following:

(1) *Shear heating.* Shear heating occurs both along the subduction thrust and volumetrically within the convecting subduction channel or mantle wedge. Volumetric shear heating is ignored in models because a maximum temperature rise of only a few °C ($\sim$1%) across a shearing, convecting layer is predicted [Turcotte and Schubert, 2002, using rates ($\sim$5 cm/yr) and viscosities ($\sim$4 $\times$ 10^{-19} Pa s), within the range anticipated for subduction zones, Gerya et al., 2002]. More comprehensive thermal mechanical models of deforming lithosphere (Burg and Gerya, 2005) also show that bulk strain outside of discrete shear zones contributes little to overall thermal structure.

Shear heating is a function of shear stress and shear velocity, and it varies with depth due to changes in rock strength. Its magnitude increases with depth to the brittle–ductile transition (e.g. Molnar and England, 1990; Leloup et al., 1999) and then decreases at greater depths as rocks weaken. Shear heating will increase temperatures adjacent to the subduction thrust – both within the top of the subducting slab and in the overlying material (mantle wedge or subduction channel). Because of this variation with depth, shear heating should produce the most heat within intermediate depths of the subduction system (e.g., 20–50 km depth), where model and rock discrepancies are largest. Shear heating is included in the models of van Keken et al. (2002) from 0 to 70 km, but not in the Gerya et al. (2002) or Syracuse et al. (2010) models. van Keken et al. (2002) do not report the magnitude of the effect of shear heating on the subduction thermal structure at shallow to intermediate depths, but an increase of as much as 25 °C is predicted for the slab top at 90–95 km depth (3 GPa).
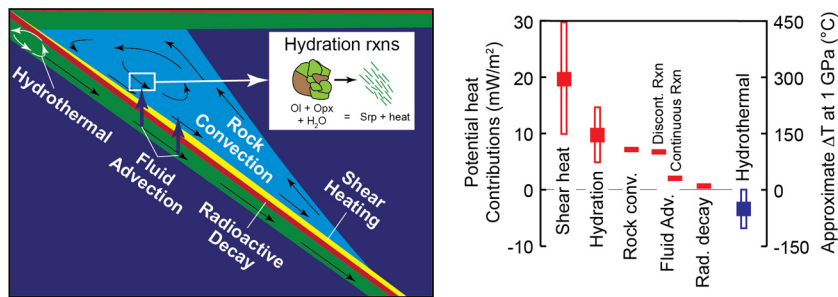
Fig. 9. Sources of heat and estimates of potential contributions to heat budgets and associated changes in temperature (ΔT) within subduction zones. ΔT is calculated at 1 GPa assuming steady-state, one-dimensional heat transfer by conduction using an average crustal thermal conductivity (2.25 W/m K). Ol = olivine, Opx = orthopyroxene, Srp = serpentine. (For interpretation of the color in this figure, the reader is referred to the web version of this article.)

Shear stresses along subduction thrusts have been proposed to range from a few tens of MPa to ~100 MPa (e.g. see Molnar and England, 1990; Peacock, 1993), and the effects of resulting shear heating can increase temperatures dramatically. A simple calculation of heat flux (shear stress multiplied by slip velocity) for a relatively low shear stress (20 MPa) and slow slip rate (30 mm/yr) provides a rough estimate of ~ 20 mW/m^2 (see Fig. 9). Some subduction models suggest that shear stresses of 65–70 MPa induce temperature increases of 250–500 °C at 35 km depth (Peacock, 1993; England and Molnar, 1993). Temperature increases of up to 200 °C at depths of greater than ~15 km are also inferred in models of other geodynamic settings, e.g. strike-slip faults and continent-continent collisions (Leloup et al., 1999; Burg and Gerya, 2005; Nabelek et al., 2010). Some shear heating must occur and could help explain the ~200–300 °C temperature disparity between models and rocks.

(2) *Convective movement of rock.* Convection of rock within the mantle or in the subduction channel can also strongly affect heat transport and temperatures. The van Keken et al. (2002) and Syracuse et al. (2010) models specify rigid crust and upper mantle at shallow levels, such that convective heat transport is effectively limited to depths greater than 80 km. This configuration ensures extremely low heat flow in the "cold nose" of the wedge, but also implies unusually low temperatures elsewhere. For example, backarc temperatures estimated from melt extraction thermometry on primitive basalts in the Cascades (Till et al., 2013) are hotter than those predicted by Syracuse et al. (2010). In contrast, convection of rock both at shallower levels within the mantle (Kelemen et al., 2003) and within the subduction channel (Gerya et al., 2002) at rates of centimeters per year contributes significantly to heat transport. Convection of rock within the subduction channel does not completely resolve model–rock disparities, but can account for much of the difference.

(3) *Mineral reactions.* None of the models considered here include the effects of metamorphic mineral reactions on the thermal structure of the subduction zone. Endothermic devolatilization reactions dominate in the subducting slab, but are thought to reduce temperatures at or below the slab top by less than 10 °C (Peacock, 1987, 1990). Dehydration of hydrated mantle is thought to reduce temperatures by as much as 75 °C, but only at depths below ~80 km (Anderson et al., 1978). Whereas this process might help explain the steepening of the geotherm between 2.5 and 4 GPa, it would not help explain anomalously hot conditions at $P < 2.5$ GPa. Conversely, fluid release from the subducting slab drives exothermic hydration and carbonation reactions in the overlying mantle wedge or subduction channel. Estimates of potential fluid flux range from ~0.1 to 0.3 kg H_2O/m^2/yr varying with convergence rate (Peacock, 1987, 1990; Gerya et al., 2002). How this fluid hydrates the overlying mantle is not completely understood. For example we do not know whether hydration reactions are localized near the subduction thrust or more generally distributed

above it. Regardless, if ~2 wt% H_2O is driven off the subducting slab continuously from 0 to 100 km depth (e.g. see Peacock, 1987, 1990; Gerya et al., 2002), and all derived H_2O is consumed at the subduction thrust, the corresponding heat flux is readily calculated. For a flux of 0.1 kg H_2O/m^2/yr (~5 moles, convergence rate of 3 cm/yr) and an enthalpy of reaction of ~30 kJ/mole H_2O for hydration reactions (Peacock, 1987) the effect of these reactions on heat flux is ~5 mW/m^2. A higher rate of convergence (10 cm/yr) would increase the heat flux to ~15 mW/m^2. At steady state, this heat flux would increase temperatures by 75–200 °C at $P \sim 1$ GPa. Such a contribution could contribute to the mismatch between rocks and the Gerya et al. (2002) and possibly the Syracuse et al. (2010) models.

(4) *Radioactive decay.* Radioactive decay contributes to the heat budget of subduction zones (e.g. Royden, 1993), and although the magnitude of its contribution is not known well, it is probably small. The concentration of heat producing elements (principally U, Th and K) in oceanic lithosphere and mantle is extremely low, so ultimately heat production depends on concentrations in subducted sediment and on the thickness of subducted sediment. Although U, Th and K concentrations may be estimated to within a factor of ~2, the thickness of subducted sediment is poorly constrained. The models of Gerya et al. (2002), van Keken et al. (2002) and Syracuse et al. (2010) assume a subducted sediment thickness of a few hundred meters. For moderate radioactive heat production in shale (2 μW/m^3; Taylor and McLennan, 1985), even a large subducted sediment thickness of 1 km would contribute <20% to heat flux. Thus, radioactive decay is likely a minor contributor to subduction zone temperatures (≤30 °C at 1 GPa), so its exclusion cannot explain the observed temperature differences between exhumed rocks and models.

(5) *Heat transport by fluids.* Fluids released during metamorphism also advect heat. While the Gerya et al. (2002) models include the rheological effects of adding H_2O to the mantle wedge, they do not include heat transport by fluids. Peacock (1987, 1990) examined the thermal effects of metamorphic fluids in detail. For continuous dehydration and pervasive flow, changes in temperature range up to a few tens of °C. If dehydration occurs due to specific discontinuous reactions (e.g. amphibole dehydration), pervasive flow can potentially increase temperatures by ~100 °C in some regions. For young subducting crust, hydrothermal flow at shallow levels of the subduction system effectively transfers heat from the subducting slab to the trench, such that the top of the slab is as much as 100 °C cooler (Spinelli and Wang, 2009). This temperature reduction propagates deep into the subduction system, and even at pressures of 1.5 GPa, temperatures can be >50 °C cooler (Spinelli and Wang, 2009). Taken together these studies suggest that fluid flow alone cannot explain the consistently large temperature mismatch between rocks and models. Although large temperature increases are possible in some specific regions, they are not uniform (whereas data indicate consistent temperature off-

sets), and some models suggest that fluid flow reduces temperatures instead of increasing them.

The main arguments levied against significant heating from other sources are that forearc heat flow and seismic attenuation are low (Peacock and Wang, 1999; van Keken et al., 2002; Syracuse et al., 2010). Seismic attenuation, however, is an indirect measure of thermal structure, and many studies show higher seismic attenuation at or above the subduction thrust than in the overlying forearc, at least to depths of ~75 km (e.g., Pozgay et al., 2009). This observation might reflect contributions from shear heating or hydration reactions along the subduction thrust. In some cases studies have argued that heat sources including shear heating (Molnar and England, 1990) or radioactive decay plus uplift (Royden, 1993) are necessary to explain heat flow measurements in the range of 35–40 mW/m^2. Shallow fluid flow within fractured basaltic crust reduces heat flow in the forearc, at least when the subducting crust is young (although it simultaneously increases heat flow at the trench; Spinelli and Wang, 2009). Heat fluxes can be reduced further by high sedimentation rates. Overall, it is difficult to verify that low heat flow and low seismic attenuation uniquely require low temperatures throughout the forearc, particularly along the subduction thrust. Insofar as shear heating, convection of rock in the subduction channel, and hydration reactions hold the greatest promise for reconciling model–rock temperature discrepancies, these factors should be considered in geodynamic models of subduction zones.

Combination of these different heat sources might lead to the markedly concave upward distribution of P_{max}–T conditions (Fig. 5) and P–T paths (Fig. 6). For example, shear heating, fluid flux and hydration reactions might plausibly be most effective at heat transfer in relatively shallow to moderate depths within the subduction system where shear stress and fluid fluxes are high. Consideration of these depth-dependent contributions to heat transfer in revised models has the potential to increase temperatures more at $P \leq 2$ GPa compared to deeper in the system.

4.3. Are anomalously hot rocks preferentially exhumed?

The rocks that are the focus of this study were not successfully subducted – they have all been exhumed and returned to the Earth's surface. Thus, it is reasonable to consider whether rocks that are returned to the surface are anomalous and hence unrepresentative of the average subduction zone. Five factors bear on the degree to which exhumed rocks represent the ambient subduction geotherm.

(1) *Thermal buoyancy due to age and speed of crust.* If thermal buoyancy facilitates the return of rocks to the Earth's surface, then rocks would record hotter conditions than expected in an average subduction zone. To evaluate this possibility, we consider two parameters that the models suggest most strongly control thermal conditions within a subduction zone: the age of the subducting oceanic crust and the convergence velocity. Evidence from exhumed rocks where these two parameters are characterized can address whether these factors can explain the relatively hot conditions recorded by the rocks.

Agard et al. (2009) compile estimates of the age of the subducting plate at the time of subduction and convergence velocity for exhumed oceanic rocks. Here, we split subduction zones into those with relatively young subducting crust (<~ 50 Ma, includes the Franciscan, Santa Catalina Island and the Cascades, Sistan, New Caledonia, Cuba, and the Dominican Republic) and those with relatively old subducting crust (>~ 50 Ma, includes Zagros, the Western Alps, Japan, Himalaya, and Ecuador; Fig. 10A; for crust age in the Himalaya, see Brookfield, 1993). Whereas rocks from subduction zones with relatively young crust do record some of the hottest P–T conditions at <2 GPa, the data points for young
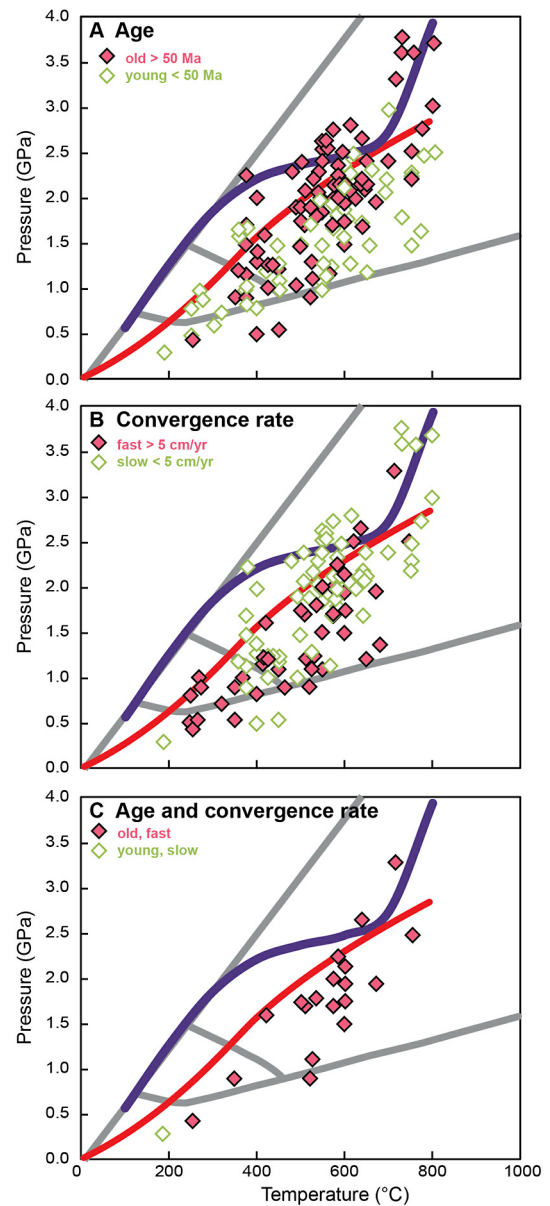

Fig. 10. Comparison of P–T estimates from paleo-subduction zones sorted by **A.** estimated age of incoming oceanic crust at the time of subduction. There is no preferential exhumation of young crust, **B.** estimated convergence velocity. There is no preferential exhumation of slowly subducting crust; **C.** both estimated age of incoming oceanic crust at the time of subduction and convergence velocity. There is no preferential exhumation of young, slow crust.

and old subducting plates largely overlap. Significantly, metamorphic rocks from subduction zones with a wide range of plate ages record P–T conditions that match models only for the youngest plate ages. Although plate age plays a role in subduction zone thermal structure, young ages alone do not appear to be responsible for the higher-T conditions recorded by rocks.

Estimates of convergence velocities are also compiled in Agard et al. (2009). Subduction zones are split here into those with relatively slow convergence velocities (<~5 cm/yr, including Cascades and the Western Alps) and relatively fast convergence (>~5 cm/yr, including Chile, Franciscan, Santa Catalina, Zagros, Himalaya, Japan, and Ecuador; Fig. 10B; for convergence velocity in the Himalaya, see Klootwijk et al., 1992). This comparison illustrates that rocks that are exhumed from subduction zones with relatively fast convergence rates appear to record similar and in some cases higher temperatures than those from subduction zones with rel-

atively slow convergence. Again, although convergence velocity likely plays a role in subduction zone thermal structures, slow convergence velocities alone do not appear to be responsible for the higher-T conditions recorded by metamorphic rocks.

Of course both plate age and convergence velocity would work in concert, so the ideal comparison is of young and slow subduction to old and fast subduction. The compiled data provide only a single data point for young crust and slow subduction (the Olympic Peninsula of the Cascades) with more data for old crust and fast subduction (Ecuador, Japan and Zagros; Fig. 10C). Even for those subduction zones that would be predicted to be the coolest (old and fast), at <2 GPa the temperatures recorded by the rocks are still hotter than the average models.

(2) *Subduction of continental crust*. Our data span both oceanic and continental subduction, so this explanation would apply to only a subset of observations. Buoyancy provided by low-density continental crust as it enters a subduction zone at the beginning of continental collision may facilitate exhumation of subduction zone rocks. Studies that have specifically modeled collision following subduction (Warren et al., 2008) predict similar P–T paths to those of subduction without collision, so it is unlikely that collision alone produced the hotter conditions preserved by rocks. Also, the ages recorded by metamorphic minerals in exhumed oceanic subduction zone rocks from the Alps are generally older than the age of continental collision (e.g. Berger and Bousquet, 2008), implying that the P–T conditions recorded by metamorphic minerals reflect normal oceanic subduction, not later collisional effects.

(3) *Subduction of asperities, hydrothermal alteration of oceanic crust, or change in geodynamic setting*. Exhumation of subduction zone rocks may be facilitated by subduction of asperities such as oceanic plateaus or seamounts (Agard et al., 2009), which is thought to have contributed to the exhumation of the Olympic blueschists (Brandon and Calderwood, 1990). The degree of hydrothermal alteration of subducted oceanic crust (creating lower density and greater buoyancy) may also drive exhumation (Angiboust and Agard, 2010). Changes in plate velocities, plate direction, and cessation of subduction may also all contribute to exhumation of materials from subduction zones (Agard et al., 2009). None of these mechanisms are expected to contribute to significantly different thermal conditions within subduction zones, however.

(4) *Subduction initiation*. Temperatures within a subduction zone at the initiation and during the early stages of subduction should be hotter than steady state subduction (e.g. Peacock, 1990). The duration for these anomalously hot conditions is likely to be relatively short, however. Models of Peacock (1990) and Kelemen et al. (2003) suggest that steady state is approached within 10–15 Ma, suggesting that rocks would be anomalously hot for even shorter time periods. Thus, if we call upon subduction initiation to explain all hotter P–T conditions for rocks, nearly all rocks exhumed from subduction zones must have been subducted within the first few Ma. Geochronologic studies in many terranes indicate that ages of protoliths and high-P metamorphism substantially postdate subduction initiation (e.g., Japan – Okamoto et al., 2004), refuting this hypothesis.

(5) *Diapiric rise from the slab interface*. Density differences between serpentinite and/or subducted sedimentary rocks compared to overlying peridotite may drive late-stage diapiric rise of material from the slab interface (e.g. Gerya and Yuen, 2003). These studies suggest that diapirs would nucleate and rise from depths of ∼65 km or greater and consequent overprinting would give rise to higher-T conditions. In contrast, our compilation of prograde P–T paths suggest that P_{max}–T conditions are not unusually warm – early stage conditions fall in the same warm P–T envelope as P_{max}–T (Fig. 6F). Diapiric rise would also require that rocks at all levels from ∼15 to 70 km experienced this process. No one has yet proposed diapiric rise over such a range of depths.

Overall, young, slow subduction zones are not preferentially exhumed: there is at least an equal representation of old, fast subduction zones in the rock record with comparable P–T distributions. Mechanisms other than thermal buoyancy are also thought to drive exhumation of some subduction-related metamorphic rocks. Therefore, even if some rocks are exhumed due to hotter conditions, it is unlikely that every exhumed metamorphic rock records anomalous subduction conditions and equally unlikely that none record "average" subduction.

5. Conclusions and implications

Our results show that metamorphic rocks exhumed from subduction zones record higher temperatures at a given depth at <∼70 km and evolve along hotter P–T trajectories than are inferred from recent geodynamic models of subduction zones. The compiled data set appears to reflect accurately the temperature at the maximum P attained by these rocks during subduction. The mismatch between models and exhumed rocks suggests that important sources of heat have been omitted in recent modeling studies of subduction zones.

The pressure–temperature history experienced by rocks within a subduction zone dictates the metamorphic reactions that occur, the depths and amounts of fluid released, and the subsequent mineral assemblages, including their volatile content. These considerations in turn determine the location and geochemistry of arc magmatism and define which elements are returned to the deep mantle. These factors are crucial to global geochemical cycles, and therefore it is essential to represent the thermal structure correctly, otherwise the subsequent interpretations fall apart.

One implication of our work is that most thermal models, especially those of Syracuse et al. (2010), appear unrepresentative of subduction systems – natural rocks are much hotter than these models at <2 GPa. Yet the models have been enormously influential as a benchmark of "typical" subduction zones and the range of P–T conditions expected for the slab top. Thus, these models serve as standards in the estimation of the global flux of H_2O in subduction zones (van Keken et al., 2011), the role of aqueous fluid in generating melts in volcanic arcs (e.g., Grove et al., 2012), the contributions of metamorphic reactions to the global carbon cycle (e.g., Ague and Nicolescu, 2014), the stability of key hydrous and petrogenetically significant minerals in subducted slabs (e.g., Baxter and Caddick, 2013), fluid speciation and trace element mobility in subduction zones (e.g., Spandler and Pirard, 2013), and the locations of subduction zone earthquakes (e.g., Abers et al., 2013). Many high-pressure experimental studies reference model slab-top P–T paths (e.g., Till et al., 2012), presumably to illustrate expected subduction zone conditions. Thus, if the cold conditions indicated by models misrepresent nature, as our compilation suggests, then many comparisons and conclusions of these complementary and derivative studies require reconsideration.

As one example, models predict that hot subduction zones, such as Cascadia, should release most of the slab's H_2O at relatively shallow levels resulting in nearly complete dehydration by 80 km depth. On the other hand, cold subduction zones, which dominate the models of Syracuse et al. (2010), are expected to retain much of their H_2O, so that overall an estimated one-third of the bound H_2O within the subducting slab reaches depths of 240 km (van Keken et al., 2011). Yet, the model P–T conditions for Cascadia are not anomalously hot compared to most subduction zone metamorphic rocks. If metamorphic rocks indeed record conditions typically experienced within subduction zones, far more H_2O is released during subduction at shallower levels, and far less H_2O has been recycled into the mantle. Therefore decarbonation and garnet growth should be faster and occur at shallower levels than currently modeled (Ague and Nico-

lescu, 2014; Baxter and Caddick, 2013; Kelemen and Manning, 2015).

Petrology and geodynamics share many goals, including the prediction of mineral assemblages that form within subduction zones because these assemblages control so many aspects of subduction zone fluid release, element recycling, seismicity, etc. There is, however, surprisingly little overlap between the mineral assemblages predicted by thermal models and the most commonly observed mineral assemblages in natural rocks. Some observed mineral assemblages and corresponding thermal conditions can perhaps be explained by phenomena like overprinting. Conversely, low surface heat flow that constrains the relatively cold model temperature distributions to $P \sim 2$ GPa can perhaps be explained by surface fluid flow in oceanic crust or high sedimentation rates. The notable absence of assemblages that record the relatively cold environments predicted by many models at shallow depths ($P \sim 0.5$ to 2 GPa) suggests that heat fluxes at these depths are underrepresented.

Acknowledgements

Appendix A. Supplementary material

Supplementary material related to this article can be found online at http://dx.doi.org/10.1016/j.epsl.2015.07.031.

References

Abers, G.A., Nakajima, J., van Keken, P.E., Kita, S., Hacker, B.R., 2013. Thermal-petrological controls on the location of earthquakes within subducting plates. Earth Planet. Sci. Lett. 369, 178–187.

Agard, P., Yamato, P., Jolivet, L., Burov, E., 2009. Exhumation of oceanic blueschists and eclogites in subduction zones: timing and mechanisms. Earth-Sci. Rev. 92, 53–79.

Ague, J.J., Nicolescu, S., 2014. Carbon dioxide released from subduction zones by fluid-mediated reactions. Nat. Geosci. 7, 355–360.

Anderson, R.N., DeLong, S.E., Schwartz, W.M., 1978. Thermal model for subduction with dehydration in the downgoing slab. J. Geol. 86, 731–739.

Angiboust, S., Agard, P., 2010. Initial water budget: the key to detaching large volumes of eclogitized oceanic crust along the subduction channel? Lithos 120, 453–474.

Ashley, K.T., Caddick, M.J., Steele-MacInnis, M.J., Bodnar, R.J., Dragovic, B., 2014. Geothermobarometric history of subduction recorded by quartz inclusions in garnet. Geochem. Geophys. Geosyst. 15, 350–360.

Baxter, E.F., Caddick, M.J., 2013. Garnet growth as a proxy for progressive subduction zone dehydration. Geology 41, 643–646.

Berger, A., Bousquet, R., 2008. Subduction-related metamorphism in the Alps: review of isotopic ages based on petrology and their geodynamic consequences. Geol. Soc. (Lond.) Spec. Publ. 298, 117–144.

Brandon, M.T., Calderwood, A.R., 1990. High-pressure metamorphism and uplift of the Olympic subduction complex. Geology 18, 1252.

Brookfield, M.E., 1993. The Himalayan passive margin from Precambrian to Cretaceous. Sediment. Geol. 84, 1–35.

Burg, J.P., Gerya, T.V., 2005. The role of viscous heating in Barrovian metamorphism of collisional orogens: thermomechanical models and application to the Lepontine Dome in the Central Alps. J. Metamorph. Geol. 23, 75–95.

Cloos, M., 1982. Flow melanges: numerical modeling and geologic constraints on their origin in the Franciscan subduction complex, California. Geol. Soc. Am. Bull. 93, 330–345.

Dragovic, B., Samanta, L.M., Baxter, E.F., Selverstone, J., 2012. Using garnet to constrain the duration and rate of water-releasing metamorphic reactions during subduction: an example from Sifnos, Greece. Chem. Geol. 314–317, 9–22.

England, P., Molnar, P., 1993. The interpretation of inverted metamorphic isograds using simple physical calculations. Tectonics 12, 145–157.

Gerya, T.V., Stockhert, B., Perchuk, A.L., 2002. Exhumation of high-pressure metamorphic rocks in a subduction channel: a numerical simulation. Tectonics 21.

Gerya, T.V., Yuen, D.A., 2003. Rayleigh–Taylor instabilities from hydration and melting propel 'cold plumes' at subduction zones. Earth Planet. Sci. Lett. 212, 47–62.

Gorman, P.J., Kerrick, D.M., Connolly, J.A.D., 2006. Modeling open system metamorphic decarbonation of subducting slabs. Geochem. Geophys. Geosyst. 7.

Groppo, C., Forster, M., Lister, G., Compagnoni, R., 2009. Glaucophane schists and associated rocks from Sifnos (Cyclades, Greece): new constraints on the P–T evolution from oxidized systems. Lithos 109, 254–273.

Grove, T.L., Till, C.B., Krawczynski, M.J., 2012. The role of H_2O in subduction zone magmatism. Annu. Rev. Earth Planet. Sci. 40, 413–439.

Hacker, B., 2006. Pressures and temperatures of ultrahigh-pressure metamorphism: implications for UHP tectonics and H_2O in subducting slabs. Int. Geol. Rev. 48, 1053–1066.

Kelemen, P.B., Manning, C.E., 2015. Reevaluating carbon fluxes in subduction zones, what goes down, mostly comes up. Proc. Natl. Acad. Sci. www.pnas.org/cgi/doi/10.1073/pnas.1507889112.

Kelemen, P.B., Rilling, J.L., Parmentier, E.M., Mehl, L., Hacker, B.R., 2003. Thermal structure due to solid-state flow in the mantle wedge beneath arcs. In: Inside the Subduction Factory. In: Geophys. Monogr., vol. 138. American Geophysical Union, pp. 293–311.

Klootwijk, C.T., Gee, J.S., Peirce, J.W., Smith, G.M., McFadden, P.L., 1992. An early India–Asia contact; paleomagnetic constraints from Ninetyeast Ridge, ODP Leg 121. Geology 20, 395–398.

Krogh Ravna, E., 2000. The garnet-clinopyroxene Fe^{2+}–Mg geothermometer: an updated calibration. J. Metamorph. Geol. 18, 211–219.

Krogh Ravna, E.J., Terry, M.P., 2004. Geothermobarometry of UHP and HP eclogites and schists – an evaluation of equilibria among garnet-clinopyroxene-kyanite-phengite-coesite/quartz. J. Metamorph. Geol. 22, 579–592.

Leloup, P.H., Ricard, Y., Battaglia, J., Lacassin, R., 1999. Shear heating in continental strike-slip shear zones: model and field examples. Geophys. J. Int. 136, 19–40.

Liou, J.G., Hacker, B.R., Zhang, R.Y., 2000. Into the forbidden zone. Science 287, 1215.

Molnar, P., England, P., 1990. Temperatures, heat flux, and frictional stress near major thrust faults. J. Geophys. Res. 95, 4833.

Nabelek, P.I., Whittington, A.G., Hofmeister, A.M., 2010. Strain heating as a mechanism for partial melting and ultrahigh temperature metamorphism in convergent orogens: implications of temperature-dependent thermal diffusivity and rheology. J. Geophys. Res. 115.

Okamoto, K., Shinjoe, H., Katayama, I., Terada, K., Sano, Y., Johnson, S., 2004. SHRIMP U–Pb zircon dating of quartz-bearing eclogite from the Sanbagawa Belt, southwest Japan: implications for metamorphic evolution of subducted protolith. Terra Nova 16, 81–89.

Peacock, S.M., 1987. Thermal effects of metamorphic fluids in subduction zones. Geology 15, 1057–1060.

Peacock, S.M., 1990. Numerical simulation of metamorphic pressure–temperature–time paths and fluid production in subducting slabs. Tectonics 9, 1197–1211.

Peacock, S.M., 1993. The importance of blueschist → eclogite dehydration reactions in subducting oceanic crust. Geol. Soc. Am. Bull. 105, 684–694.

Peacock, S.M., Wang, K., 1999. Seismic consequences of warm versus cool subduction metamorphism: examples from Southwest and Northeast Japan. Science 286, 937–939.

Powell, R., 1985. Regression diagnostics and robust regression in geothermometer/geobarometer calibration: the garnet-clinopyroxene geothermometer revisited. J. Metamorph. Geol. 3, 231–243.

Pozgay, S.H., Wiens, D.A., Conder, J.A., Shiobara, H., Sugioka, H., 2009. Seismic attenuation tomography of the Mariana subduction system: implications for thermal structure, volatile distribution, and slow spreading dynamics. Geochem. Geophys. Geosyst. 10.

Royden, L.H., 1993. The steady state thermal structure of eroding orogenic belts and accretionary prisms. J. Geophys. Res. 98, 4487.

Schmädicke, E., Will, T.M., 2003. Pressure–temperature evolution of blueschist facies rocks from Sifnos, Greece, and implications for the exhumation of high-pressure rocks in the Central Aegean. J. Metamorph. Geol. 21, 799–811.

Spandler, C., Pirard, C., 2013. Element recycling from subducting slabs to arc crust: a review. Lithos 170–171, 208–223.

Spear, F., 1993. Metamorphic Phase Equilibria and Pressure–Temperature–Time Paths. Mineralogical Society of America, Washington, DC.

Spear, F.S., Wark, D.A., Cheney, J.T., Schumacher, J.C., Watson, E.B., 2006. Zr-in-rutile thermometry in blueschists from Sifnos, Greece. Contrib. Mineral. Petrol. 152, 375–385.

Spinelli, G.A., Wang, K., 2009. Links between fluid circulation, temperature, and metamorphism in subducting slabs. Geophys. Res. Lett. 36.

Syracuse, E.M., Abers, G.A., 2006. Global compilation of variations in slab depth beneath arc volcanoes and implications. Geochem. Geophys. Geosyst. 7.

Syracuse, E.M., van Keken, P.E., Abers, G.A., 2010. The global range of subduction zone thermal models. Phys. Earth Planet. Inter. 183, 73–90.

Taylor, S.R., McLennan, S.M., 1985. The Continental Crust – Its Composition and Evolution: An Examination of the Geochemical Record Preserved in Sedimentary Rocks. Blackwell, Oxford, UK.

Till, C.B., Grove, T.L., Carlson, R.W., Donnelly-Nolan, J.M., Fouch, M.J., Wagner, L.S., Hart, W.K., 2013. Depths and temperatures of <10.5 Ma mantle melting and the lithosphere–asthenosphere boundary below southern Oregon and northern California. Geochem. Geophys. Geosyst. 14, 864–879.

Till, C.B., Grove, T.L., Withers, A.C., 2012. The beginnings of hydrous mantle wedge melting. Contrib. Mineral. Petrol. 163, 669–688.

Trotet, F., Vidal, O., Jolivet, L., 2001. Exhumation of Syros and Sifnos metamorphic rocks (Cyclades, Greece). New constraints on the P–T paths. Eur. J. Mineral. 13, 901–920.

Turcotte, D.L., Schubert, G., 2002. Geodynamics, 2nd ed. Cambridge University Press, Cambridge.

van Keken, P.E., Hacker, B.R., Syracuse, E.M., Abers, G.A., 2011. Subduction factory: 4. Depth-dependent flux of H_2O from subducting slabs worldwide. J. Geophys. Res. 116.

van Keken, P.E., Kiefer, B., Peacock, S.M., 2002. High-resolution models of subduction zones: implications for mineral dehydration reactions and the transport of water into the deep mantle. Geochem. Geophys. Geosyst. 3, 1056.

Wada, I., Wang, K., 2009. Common depth of slab-mantle decoupling: reconciling diversity and uniformity of subduction zones. Geochem. Geophys. Geosyst. 10.

Warren, C.J., Beaumont, C., Jamieson, R.A., 2008. Formation and exhumation of ultra-high-pressure rocks during continental collision: role of detachment in the subduction channel. Geochem. Geophys. Geosyst. 9.

Whitney, D.L., Davis, P.B., 2006. Why is lawsonite eclogite so rare? Metamorphism and preservation of lawsonite eclogite, Sivrihisar, Turkey. Geology 34, 473.